ACTA IMEKO
ISSN: 2221-870X
March 2018, Volume 7, Number 1, 36-41

Analysis of the magnetic field in the presence of linear sub-surface cracks using ECT

Dario J. Pasadas, Artur L. Ribeiro, Helena G. Ramos

Instituto de Telecomunicações and Instituto Superior Técnico/Universidade Técnica de Lisboa, Av. Rovisco Pais 1, 1049-001 Lisbon,Portugal

ABSTRACT
This manuscript reports a study concerning the penetration of eddy currents in metallic non-ferromagnetic materials in the presence of linear sub-surface cracks. Simulations were performed for a set of different lengths and depths of the crack using a sinusoidal excitation current with uniform magnetic field distribution. The perturbed magnetic field components (B_x and B_z) that occur due to the presence of cracks were obtained to understand the electromagnetic phenomena involved. The end and center of the crack were analyzed by the magnitude and the complex signature of the obtained magnetic field. The dependences between the length and depth of the crack and both magnetic field components were discussed.

Section: RESEARCH PAPER

Keywords: non-destructive testing; eddy current testing; sub-surface cracks; aluminium

Citation: Dario J. Pasadas, Artur L. Ribeiro, Helena G. Ramos, Analysis of the magnetic field in the presence of linear sub-surface cracks using ECT, Acta IMEKO, vol. 7, no. 1, article 7, March 2017, identifier: IMEKO-ACTA-07 (2017)-01-07

Section Editor: Lorenzo Ciani, University of Florence, Italy

Received September 29, 2017; **In final form** November 29, 2017; **Published** March 2018

Corresponding author: Dario J. Pasadas e-mail: dpasadas@lx.it.pt

1. INTRODUCTION

Eddy current testing (ECT) is a widely used non-destructive testing (NDT) technique for the inspection of cracks in conductive materials [1], without damaging the structural integrity of those materials under inspection. This technique can be applied to several industries, such as aircraft structures [2] and petrochemical pipelines [3]. Due to the complexity of the evaluation process, ECT instruments with extended capabilities for NDT inspection of materials are actively researched [4], [5].

The ECT technique is based on electromagnetic induction phenomena. It can be applied to detect and characterize surface and sub-surface cracks with a minimum preparation of the surfaces under inspection [6]-[8].

The eddy currents can be induced in the conductor by sinusoidal, pulsed or velocity excitation. A primary magnetic field is created by imposing a time-varying current in a coil. In the proximity of the coil to a metal, eddy currents are induced. A secondary magnetic field is created by the eddy currents which contains information about the state of the material.

Due to the nature of the electromagnetic phenomena, the main disadvantage of this technique is related to its limited sub-surface crack detection and characterization at deeper levels [9]. The eddy currents that flow in the metallic structure are sensitive to several factors, such as the material properties (electrical conductivity and magnetic permeability), the test frequency, the lift-off effect, the edge effect and the dimensions of the crack [10]-[11]. The flow of eddy currents in a conductor is maximum at the material surface and it is attenuated with increasing depth.

For lower electrical conductivity or low magnetic permeability of non-ferromagnetic materials, the eddy current achieves deeper penetration. For a given material, the standard penetration depth (δ) is the depth at which the current density decreases to 1/e of the surface density amplitude [12], [13], when a uniform field is applied at the material surface.

Nowadays, tools like artificial neural networks or other classification methods based on automatic machine learning algorithms have been introduced in the research field to estimate the dimensions of cracks [14], [15], but they are still in development. In this kind of methods, the determination of features is essential for the success of the estimation of defect dimensions from the measured signals. For this purpose, it is essential to study the parameters that influence the penetration

depth of the electromagnetic field into a conductive material when surface or sub-surface cracks exist. Hence, this paper presents simulation and experimental work to investigate the penetration of eddy currents in the material when a coil is excited by a sinusoidal current with uniform magnetic field distribution to evaluate sub-surface cracks. The tests were performed for linear cracks with different lengths and depths.

2. NUMERICAL MODEL AND CONDITIONS OF TEST

The simulations were computed for a 1050 aluminum alloy plate with 4 mm of thickness. Linear cracks with fixed width of 1 mm, but different lengths and depths were studied. The simulations were performed using a 2D spatially invariant excitation field with sinusoidal time variation. The excitation, in simulation and experimentally, was applied by a planar coil at a fixed lift-off distance of 0.5 mm.

The Finite Element Method software COMSOL® Multiphysics was used to evaluate the magnetic field components (B_x and B_z) in the proximity of the metallic plate containing sub-surface cracks. The physics used in this model was Magnetic Fields (AC/DC Module) with a frequency domain study type. A parametric sweep of the length and depth of the sub-surface defects were used in this study. The excitation was performed by imposing a uniform surface electromotive force.

The type of mesh elements used in this model was tetrahedral. To obtain the magnetic field components, a series of probing points along a straight line was added at 2.2 mm above the surface of the plate. A small air block, as shown in Figure 1, was created surrounding the points where the magnetic field components were computed. The air block was meshed with high density elements in order to improve the accuracy of the results and minimize the error due to the interpolation. Figure 1 depicts the defect, the air block and the measurement points used in the model.

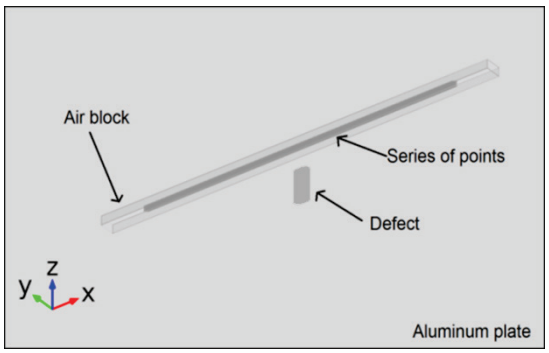

Figure 1. – Illustration of the defect, air block and series of probing points used in the model.

3. EDDY CURRENT DISTRIBUTION

The eddy currents generated inside the aluminum plate were spatially uniform inside the restricted area of planes parallel to the surface, as depicted in Figure 2(a), when no cracks are present. The eddy currents close outside the indicated region. In the proximity of a crack, the eddy current distribution is perturbed and the magnetic field produced by the eddy currents changes, as depicted in Figure 2(b). The magnetic field is sensed by a magnetic sensor located in the proximity of the crack region. Sensing coils can be used as sensing elements to detect cracks near the surface under inspection. However, their use as sensing element is insufficient to detect deep sub-surface cracks because the sensitivity of a coil is proportional to the operating frequency. Other sensors, such as superconducting quantum interference devices (SQUID), Hall effect, anisotropic magnetoresistors (AMR) or giant magnetoresistors (GMR), have been introduced in eddy current systems giving better sensitivity to detect sub-surface cracks at deeper levels [16]. Using these magnetic sensors, the perturbed magnetic field originated by the presence of a crack inside the metal is the measured quantity which is obtained to evaluate the size of the cracks. The measurements are obtained around the crack region above the surface of the metal under inspection.

In the simulations, the perturbed magnetic field components (B_x and B_z) were obtained on the top of the aluminum plate in a straight line above the linear cracks region. The distance z considered between the measurement points and the sample plate was 2.2 mm. The B_x component contains the excitation magnetic field (B_{ext}) and the perturbed magnetic field originated by the crack presence (B_{ec}), where the B_{ext} and the B_{ec} components are oppositely aligned vectors. The B_z component is zero when the aluminum plate is without cracks, and non-zero when the plate contains cracks. Thus, this means that the B_z component contains only information about the perturbed magnetic field originated by the presence of a crack in the metallic plate.

For the inspection of sub-surface cracks in metallic plates, an accurate choice of the operating frequency allows the primary magnetic field to penetrate more inside the conductor. For the 1050 aluminum alloy plate with 4 mm of thickness, a sinusoidal excitation was applied with an operating frequency (f) of 440 Hz in order to allow the eddy currents achieve deeper penetration in the material. This frequency was chosen based on the standard penetration depth (δ) for this material, and computed using the following relation:

$$f = \frac{1}{\delta^2 \mu \sigma \pi} \tag{1}$$

where the conductivity (σ) is 3.57×10^7 S/m and the permeability (μ) is $4\pi\times10^{-7}$ H/m.

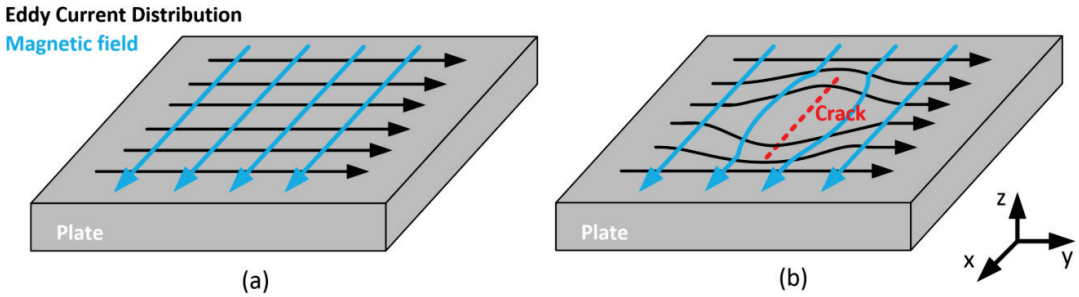

Figure 2. Representation of the eddy current flow: (a) without defect presence; (b) with defect presence.

At this operating frequency, the standard penetration depth is 4 mm, which means that the flow of eddy currents at that depth is 1/e times the maximum current density at the material surface.

For this value of the penetration depth in the aluminium plate under study, the chosen operating frequency and lift-off, the magnetic field response above the crack region is expected to be strongly dependent on the dimensions of the crack. Taking this into account, in the next section, the two obtained magnetic field components (B_x and B_z) are presented and their dependence on the length and depth of the cracks are analysed.

4. RESULTS

The simulations were performed for two crack depths (1 mm and 3 mm), and for fourteen different lengths (between 4 mm to 30 mm with an incremental step of 2 mm), as depicted in Figure 3, in order to study the eddy current density depth profile when sub-surface cracks exist in conductive materials. The depth and the length of the crack are denoted by d and l, respectively. The thickness (t) of the aluminum plate and the standard penetration depth (δ) are equal to 4 mm. The simulations and the experimental tests were carried out for fixed excitation current amplitude of 200 mA.

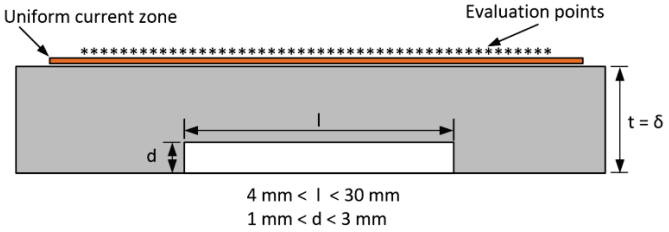

Figure 3. Cross section view in the x-z plane at the crack position.

From the simulations results, Figure 4 depicts the magnitude of the magnetic field components B_x and B_z obtained in a series of points in a straight line of 40 mm above the crack region. This straight line was placed in the region where maximum magnitude of the magnetic field perturbation is obtained in presence of a linear defect.

The results show clearly the changes of the magnetic field response due to the variation of the dimensions of the crack. It is possible to say that both magnetic field components contain information about the size of the crack and both fields allow the estimation of the position of the cracks.

For each crack size, it is possible to observe that the perturbed magnetic field B_z contains two peaks at the positions of the crack ends. The center of the defect is located at the mid-

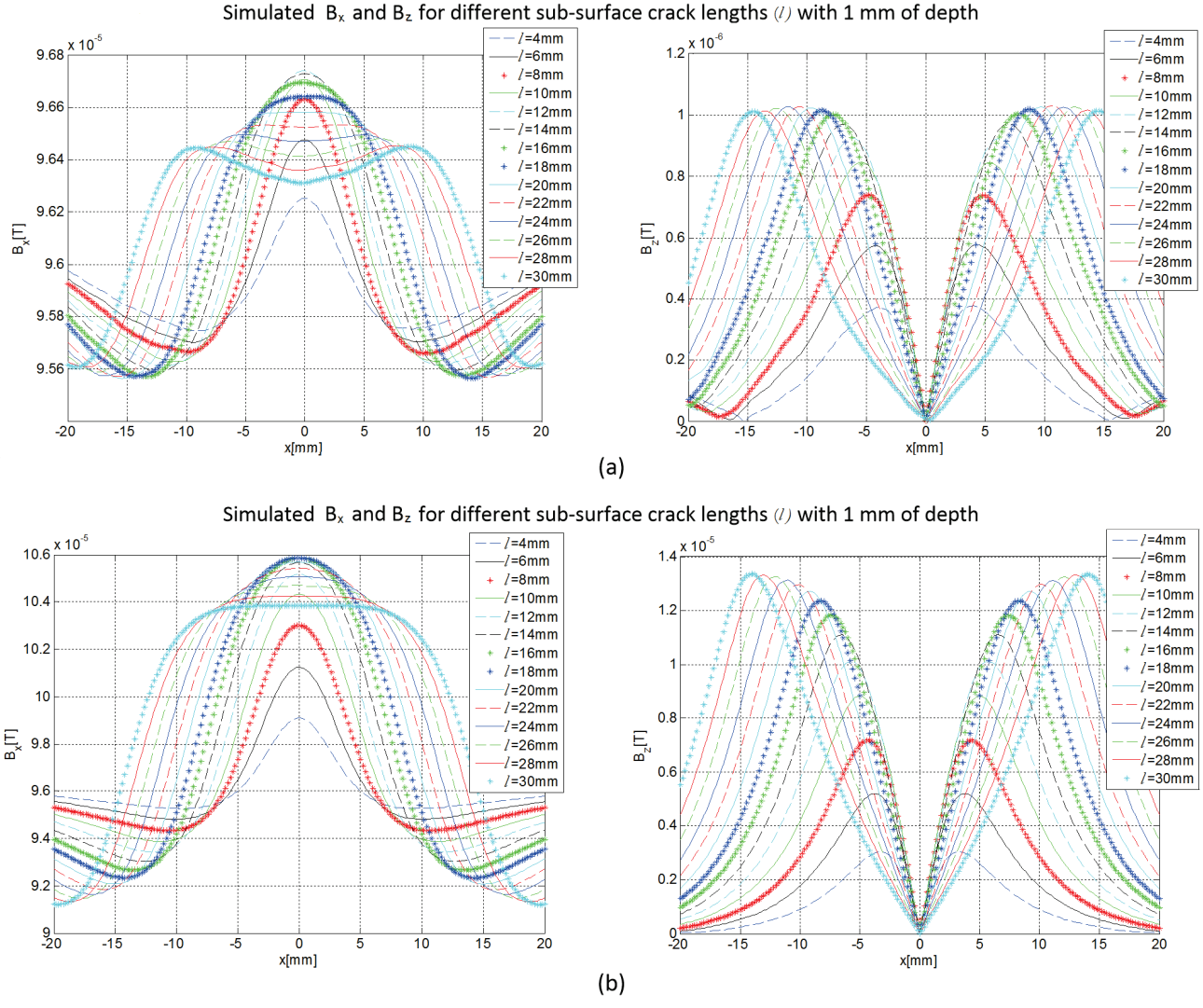

Figure 4. Simulated results of B_x and B_z obtained in a straight line above a set of different crack lengths (l); (a) Cracks depth equal to 1 mm; (b) Cracks depth equal to 3 mm.

point between the peaks of the magnitude of B_z. It is also possible to see that the magnitude of B_z, at the crack ends, is directly related with the length and depth. For long sub-surface cracks with 1 mm of depth, the magnitude of B_z tends to a constant value at the ends of the crack. If the depth of the crack increases, the same effect occurs but the magnitude of B_z tends to a constant value for much longer cracks. Concerning the magnitude of the perturbed magnetic field component B_x, the obtained results indicate that the shape of the magnetic field response at the center of the crack changes when the length of the crack increases.

In order to explain these phenomena, the peak value of B_x and B_z in function of the crack length were extracted and plotted in Figure 5. Figure 5(a) and Figure 5(b) depict the peak values of B_x and B_z for a crack depth of 1 mm and of 3 mm, respectively. From Figure 5(a), it can be seen that the peak value of the magnitude of B_x increases with respect to the length of the crack up to 12 mm. This means that a lower eddy current density region exists above the centre region of the crack, which causes an increase in the resulting magnitude of the B_x component (due to the decrease of B_{cc}). This effect is reversed for long sub-surface cracks. From Figure 5(a), it can be seen that the peak value of the magnitude of B_x decreases when the crack length increases beyond 12 mm (point of inversion). This occurs because the eddy currents that flow around the crack tend to flow above the crack. This means that the upper layer of the centre region of the crack becomes the path of lower resistance for the eddy currents. It can also be observed that the peak value of B_z increases when the crack length increases up to 12 mm (knee point). Beyond this crack length, the peak value of the magnitude of B_z tends to a constant value.

Comparing B_x and B_z, it is possible to observe that the point of inversion of the peak value of B_x curve matches approximately the knee point of the B_z curve. Taking this into account, it is possible to conclude that the amount of eddy currents that flow around/above the sub-surface cracks can be estimated from the obtained magnetic field by the length/depth ratio of the crack. However, it is important to mention that this ratio changes if the operating frequency changes. The measurement of just one component of the magnetic field is not enough to evaluate the length/depth of the crack if the peak values of the magnetic field components are considered. As an example, from Figure 5(a), if the peak value of the B_x component is equal to 9.66×10^{-4} T, it can be seen that the length of the crack has two solutions (8 mm and 18 mm). Thus, to evaluate a crack in conductive materials both components of magnetic field (B_x and B_z) provide complementary information and both fields should be considered.

From Figure 5 (b), it is possible to observe that when the depth of the crack increases, the same effect occurs but the magnitude of B_z tends to a constant value for cracks with longer length. Still in the case of Figure 5 (b), the B_x component has two corresponding solutions when the length of the crack is equal to 10 mm or 28 mm.

Experimental results were obtained with similar conditions using a measurement system with an attached planar probe to measure the magnetic field in the presence of linear sub-surface cracks. The experimental setup is described in [17]. A planar coil was used to impose uniform current distribution in the aluminium plate. Two GMR sensors were positioned in the

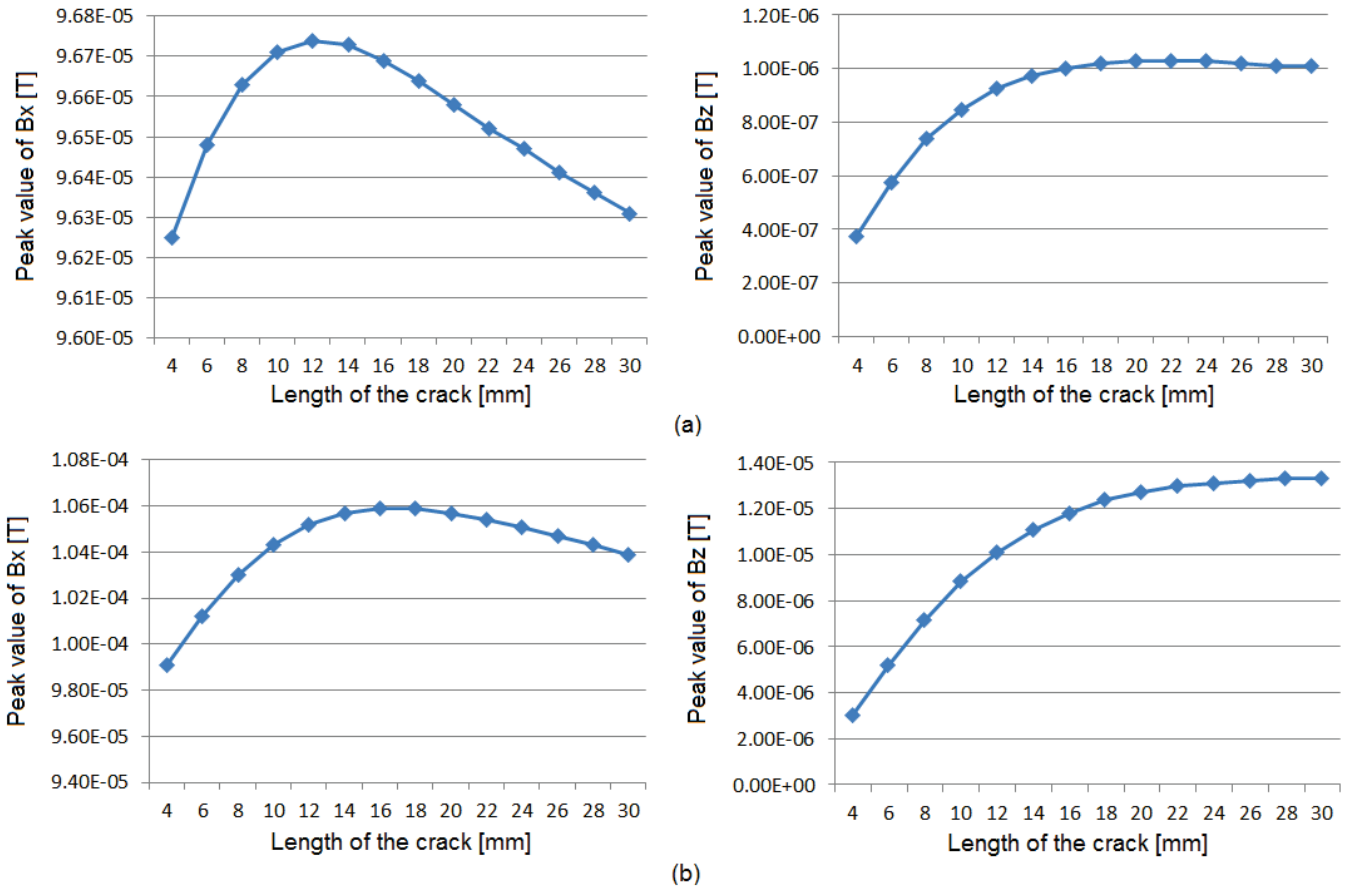

Figure 5. Peak value of B_x and B_z with respect to the crack length; (a) for a crack depth of 1 mm; (b) for a crack depth of 3mm.

centre of the coil to measure the B_x and B_z components. Figure 6 presents the components of the magnetic field (B_x and B_z) obtained experimentally for two linear sub-surface cracks with lengths of 12 mm and 8 mm at a fixed depth of 3 mm.

Comparing the experimental and the simulated results, it can be seen that the signatures of the magnitude of the magnetic field components (B_x and B_z) are similar. However, there is a mismatch between the two peak values of the B_z component. This is due to the small misalignment between the sensor and the crack orientation during the scan. For the B_x component, a baseline mismatch between the simulation and experimental results occurred because the GMR sensor was not exactly parallel to the excitation magnetic field in order to measure the strong B_x component. This small misalignment of the sensor causes a decrease in the value of magnitude measured by the GMR sensor.

From the simulations, the complex signatures of the magnetic field components were also obtained. Figure 7 depicts the complex signatures (from B_z) obtained crossing the center of all sub-surface defect length. The results are presented for two crack depths (1 mm and 3 mm).

In Figure 7, the simulated results show that the information

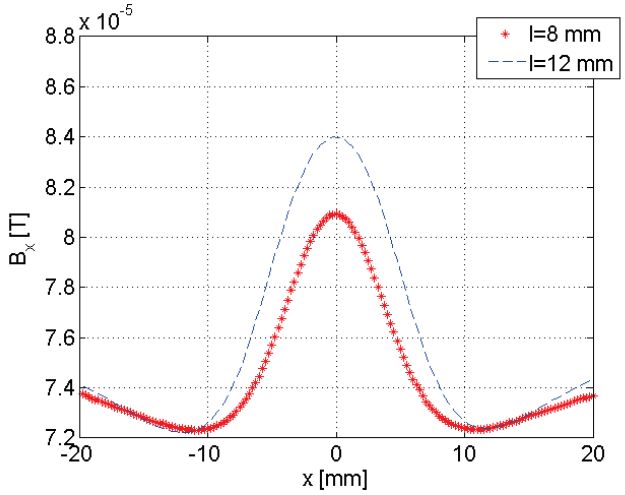

Figure 6. Experimental results of B_x and B_z obtained in a straight line above the linear sub-surface crack at a fixed depth of 3 mm and two length of 8 mm and 12 mm: (a) B_x magnetic field component ; (b) B_z magnetic field component.

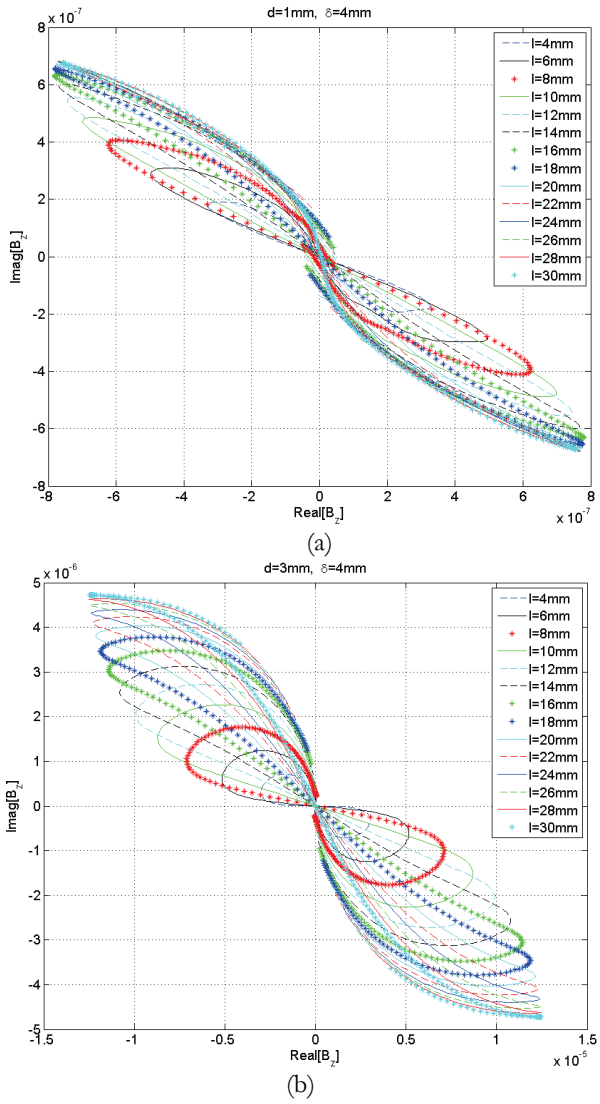

Figure 7. Simulated results of the complex signatures of B_z obtained in a straight line above linear cracks having various lengths (l): (a) Cracks depth equal to 1 mm; (b) Cracks depth equal to 3 mm.

regarding the length of the defect can be evaluated from the complex signature of the magnetic fields components B_z. In both cases, the results show that the shape of the signature changes when defect length also changes. This means that the area of each signature could be considered as a feature and calculated to estimate the crack length.

5. CONCLUSIONS

Simulations and experimental tests were performed on aluminum samples for eddy current studies. The penetrations of eddy currents in the material when a coil is excited by a sinusoidal current with uniform magnetic field distribution were studied and presented in this manuscript for sub-surface linear cracks. For a pre-defined excitation current amplitude and frequency, the eddy current penetration strongly depends on the dimensions of the crack.

The results show that the peak values of the magnetic field components (B_x and B_z) contain information about the crack. However, the measurement of only one component of the magnetic field is insufficient to evaluate the length and depth of the crack. This is mainly because the eddy currents tend to flow

in the least resistance path, which has a dependence on the dimensions of the crack. This means that both magnetic field components (B_x and B_z) should be considered to evaluate cracks in metallic structures.

Concerning the obtained complex signatures of B_z, the results showed that the shape of the signatures changes when the defect length changes. For a pre-defined excitation current amplitude and frequency, this feature can be useful to classify the length and depth of the sub-surface defect in a range of known geometries of the defect.

ACKNOWLEDGEMENT

This work was supported in part by Project UID/EEA/50008/2013 - RELIM and the Project FCT PTDC/EEI-ELC/5811/2014. This support is gratefully acknowledged.

REFERENCES

[1] J. G. Martín, J. G. Gil, E. V.-Sánchez, "Non-destructive techniques based on eddy current testing", Sensors, 2011, Vol. 11, pp. 2525–2565.

[2] G. Yang, Z. Zeng, Y. Deng, X. Liu, L. Udpa, A. Tamburrino, S.S. Udpa, "3D EC-GMR sensor system for detection of subsurface defects at steel fastener sites", NDT&E International, Vol. 50, 2012, pp. 20-28.

[3] M. Coramik, Y. Ege, "Discontinuity inspection in pipelines: A comparison review", Measurement, 2017, Vol. 111, pp. 359-373.

[4] D. Pasadas, T. Rocha, H. G. Ramos, A. L. Ribeiro, "Evaluation of portable ECT instruments with positioning capability", Measurement, January, 2012, Vol. 45, No. 1, pp. 393-404.

[5] D. E. Aguiam, L. S. Rosado, P. M. Ramos, M. Piedade, "Heterodyning based portable instrument for eddy currents non-destructive testing", Measurement, September, 2015, Vol. 45, pp. 146-157.

[6] J. H. Espina-hernánez, E. Ramírez-Pacheco, F. Caleyo, J. A. Pérez Benitez, J. M. Hallen, "Rapid estimation of artificial near-side crack dimensions in aluminium using a GMR-based eddy current sensor", NDT & E International, October, 2012, Vol. 51, No. 1, pp. 94-100.

[7] D. J. Pasadas, A. L. Ribeiro, H. G. Ramos, T. J. Rocha, "Inspection of Cracks in Aluminum Multilayer Structures Using Planar ECT Probe and Inversion Problem", IEEE Trans. Instrum. Meas., May, 2017, Vol. 66, No. 5, pp. 920-927.

[8] Y-J Kim, S-S Lee, "Eddy current probes of inclined coils for increased detectability of circumferential cracks in tubing", NDT & E International, July, 2012, Vol. 49, pp. 77-82.

[9] B. P. C. Rao, "Practical Eddy Current Testing", Alpha Science International Ltd, 2007.

[10] J. García-Martín, J. Gómez-Gil, E. Vázquez-Sánchez, "Non Destructive Techniques Based on Eddy Current Testing", Sensors, 2011, Vol. 11, pp. 2525-2565.

[11] M. Ricci, G. Silipigni, L. Ferrigno, M. Laracca, I. D. Adewalea, G. Y. Tian, "Evaluation of the lift-off robustness of eddy current imaging techniques", NDT & E International, January, 2017, Vol. 85, pp. 43-52.

[12] J. Kral, R. Smid, H. M. G. Ramos, A. L. Ribeiro, "The Lift-Off Effect in Eddy Currents on Thickness Modeling and Measurement", IEEE Trans. on Instr. and Meas., 2013, Vol. 62, No. 7, pp. 2043 - 2049.

[13] A. Bernieri, G. Betta, L. Ferrigno, M. Laracca, "Multi frequency ECT method for defect depth estimation", IEEE Sensors Applications Symposium, February, 2012.

[14] A. Bernieri, G. Betta, L. Ferrigno, M. Laracca, S. Mastrostefano. "Multifrequency Excitation and Support Vector Machine Regressor for ECT Defect Characterization", IEEE Trans. Instrum. Meas., 2014, Vol. 63, No. 5, pp. 1272-1280.

[15] J. Kim, G. Yang, L. Udpa, S. Udpa, "Classification of pulsed eddy current GMR data on aircraft structures", NDT& E International, 2010, Vol. 43, No. 2, pp.141-144.

[16] H. G. Ramos, A. L. Ribeiro, "Present and Future Impact of Magnetic Sensors in NDE", Procedia Engineering, 2014, Vol. 86 pp. 406-419.

[17] D. J. Pasadas, A. L. Ribeiro, T. Rocha, H. G. Ramos, "2D surface defect images applying Tikhonov regularized inversion and ECT", NDT& E International, 2016, Vol. 80 pp. 48-57.